# Thermodynamic limit from small lattices of coupled maps

R. Carretero-González[1,*], S. Ørstavik[1], J. Huke[2], D.S. Broomhead[2] and J. Stark[1]
[1] *Centre for Nonlinear Dynamics and its Applications*[†], *University College London, London WC1E 6BT, U.K.*
[2] *Department of Mathematics, University of Manchester Institute of Science & Technology, Manchester M60 1QD, U.K.*
(Submitted to Phys. Rev. Lett, March 1999)

We compare the behaviour of a small truncated coupled map lattice with random inputs at the boundaries with that of a large deterministic lattice essentially at the thermodynamic limit. We find exponential convergence for the probability density, predictability, power spectrum, and two-point correlation with increasing truncated lattice size. This suggests that spatio-temporal embedding techniques using local observations cannot detect the presence of spatial extent in such systems and hence they may equally well be modelled by a local low dimensional stochastically driven system.

PACS numbers: 05.45.Ra, 05.45.Jn, 05.45.Tp

Observation plays a fundamental role throughout all of physics. Until this century, it was generally believed that if one could make sufficiently accurate measurements of a classical system, then one could predict its future evolution for all time. However, the discovery of chaotic behaviour over the last 100 years has led to the realisation that this was impractical and that there are fundamental limits to what one can deduce from finite amounts of observed data. One aspect of this is that high dimensional deterministic systems may in many circumstances be indistinguishable from stochastic ones. In other words, if we have a physical process whose evolution is governed by a large number of variables, whose precise interactions are a priori unknown, then we may be unable to decide on the basis of observed data whether the system is fundamentally deterministic or not. This has led to an informal classification of dynamical systems into two categories: low dimensional deterministic systems and all the rest. In the case of the former, techniques developed over the last two decades allow the characterisation of the underlying dynamics from observed time series via quantities such as fractal dimensions, entropies and Lyapunov spectra [1]. Furthermore, it is possible to predict and manipulate such time series in highly effective ways with no prior knowledge of the physical system generating the data. In the case of high dimensional and/or stochastic systems, on the other hand, relatively little is known about what information can be extracted from observed data, and this topic is currently the subject of intense research.

Many high dimensional systems have a spatial extent and can best be viewed as a collection of subsystems at different spatial locations coupled together.The main aim of this letter is to demonstrate that using data observed from a limited spatial region we may be unable to distinguish such an extended spatio-temporal system from a local low dimensional system driven by noise. Since the latter is much simpler, it may in many cases provide a preferable model of the observed data. On one hand this suggests that efforts to reconstruct by time delay embedding the spatio-temporal dynamics of extended systems may be misplaced, and we should instead focus on developing methods to locally embed observed data. A preliminary framework for this is described in [2]. On the other hand, these results may help to explain why time delay reconstruction methods sometimes work surprisingly well on data generated by high dimensional spatio-temporal systems, where a priori they ought to fail: in effect such methods only see a "noisy" local system, and providing a reasonably low "noise level" can still perform adequately. Overall we see that we add a third category to the above informal classification: namely that of low dimensional systems driven by noise and we need to adapt our reconstruction approach to take account of this.

We present our results in the context of coupled map lattices (CML's) which are a popular and convenient paradigm for studying spatio-temporal behaviour [3]. In particular, consider a one-dimensional array of diffusively coupled logistic maps:

$$x_i^{t+1} = (1-\varepsilon) f(x_i^t) + \frac{\varepsilon}{2}(f(x_{i-1}^t) + f(x_{i+1}^t)), \qquad (1)$$

where $x_i^t$ denotes the discrete time dynamics at discrete locations $i = 1, \ldots, L$, $\varepsilon \in [0,1]$ is the coupling strength and the local map $f$ is the fully chaotic logistic map $f(x) = 4x(1-x)$. Recent research has focused on the thermodynamic limit, $L \to \infty$, of such dynamical systems [4]. Many interesting phenomena arise in this limit, including the rescaling of the Lyapunov spectrum [5] and the linear increase in Lyapunov dimension [6]. The physical interpretation of such phenomena is that a long array of coupled systems may be thought of as a concatenation of small-size sub-systems that evolve almost independently from each other [7]. As a consequence, the limiting behaviour of an infinite lattice is extremely well approximated by finite lattices of quite modest size. In our numerical work, we thus approximate the thermodynamic limit by a lattice of size $L = 100$ with periodic boundary conditions.

Numerical evidence [2] suggests that the attractor in such a system is high-dimensional (Lyapunov dimension approximately 70). If working with observed data it is clearly not feasible to use an embedding dimension of that order of magnitude. On the other hand, it is possible [2] to make quite reasonable predictions of the evolution of a site using embedding dimensions as small as 4. This suggests that a significant part of the dynamics is concentrated in only a few degrees of freedom and that a low dimensional model may prove to be a good approximation of the dynamics at a single site. In order to investigate this we introduce the following truncated lattice. Let us take $N$ sites ($i = 1, \ldots, N$) coupled as in equation (1) and consider the dynamics at the boundaries $x_0^t$ and $x_{N+1}^t$ to be produced by two independent driving inputs. The driving input is chosen to be white noise uniformly distributed in the interval $[0, 1]$. We are interested in comparing the dynamics of the truncated lattice to the thermodynamic limit case.

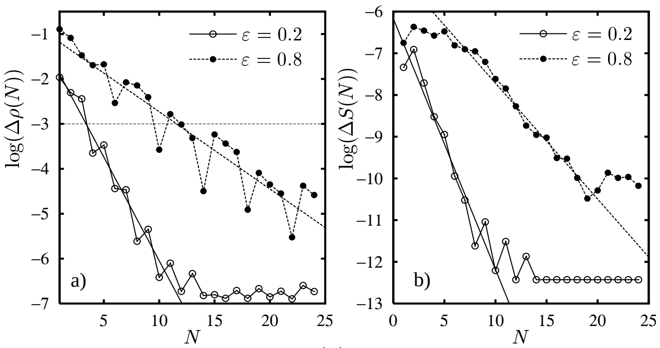


FIG. 1. Distance between (a) the probability density and (b) the power spectra in the thermodynamic limit and its truncated lattice counterpart as the number of sites $N$ in the latter is increased.

We begin the comparison between the two lattices by examining their respective invariant probability density at the central site (if the number of sites is even, either of the two central sites is equivalent). For a semi-analytic treatment of the probability density of large arrays of coupled logistic maps see Lemaître *et al.* [8]. Let us denote by $\rho_\infty(x)$ the single site probability density in the thermodynamic limit and $\rho_N(x)$ the central site probability density of the truncated lattice of size $N$. We compare the two densities in the $\mathcal{L}_1$ norm by computing

$$\Delta\rho(N) = \int_0^1 |\rho_\infty(x) - \rho_N(x)|\, dx \qquad (2)$$

for increasing $N$. The results are summarised in figure 1.a where $\log(\Delta\rho(N))$ is plotted for increasing $N$ for different values of the coupling. The figure suggests that the difference between the densities decays exponentially as $N$ is increased (see straight lines for guidance). Similar results were obtained for intermediate values of the coupling parameter. The densities used to obtain the plots in figure 1.a were estimated by a box counting algorithm by using 100 boxes and $10^8$ points ($10^2$ different orbits with $10^6$ iterations each). The maximum resolution typically achieved by using these values turns to be around $\Delta\rho(N) \simeq \exp(-6.5) \simeq 0.0015$. This explains the saturation of the distance corresponding to $\varepsilon = 0.2$. For $\varepsilon = 0.8$ the saturation would occur for approximately $N = 30, 35$ given enough computing power (more refined boxes and more iterations). Nonetheless, densities separated by a distance of approximately $\exp(-3) \simeq 0.05$ (see horizontal threshold in figure 1.a), or less, capture almost all the structure. Therefore, one recovers the essence of the thermodynamic limit probability density with a reasonable small truncated lattice (see figures 2.a,b).

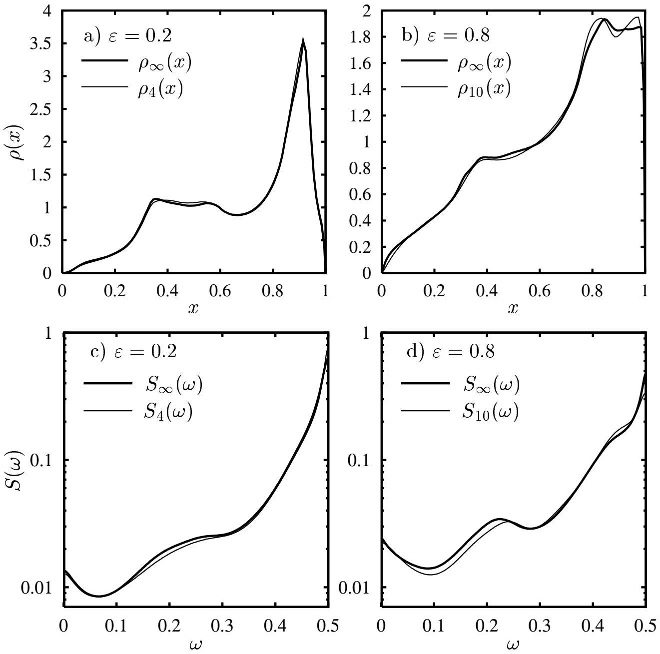


FIG. 2. Approximating (a,b) the probability density and (c,d) the power spectra of the thermodynamic limit (thick lines) using a truncated lattice (thin lines).

Next we compare temporal correlations in the truncated lattice with those in the full system. Denote by $S_\infty(\omega)$ the power spectrum of the thermodynamic limit and $S_N(\omega)$ its counterpart for the truncated lattice. Figure 1.b shows the difference $\Delta S(T)$ in the $\mathcal{L}_1$ norm between the power spectra of the truncated lattice and of the thermodynamic limit for $\varepsilon = 0.2$ and 0.8 (similar results were obtained for intermediate values of $\varepsilon$). As for the probability density, the power spectra appear to converge exponentially with the truncated lattice size. Note that for large $N$, particularly for small $\varepsilon$, the difference tends to saturate around $\exp(-12) \approx 10^{-6}$, this is because the accuracy of our power spectra computations reaches its limit (with more iterations one can reduce the effects of the saturation). Our results were obtained by averaging $10^6$ spectra ($|\mathrm{DFT}|^2$) of 1024 points each. In figures 2.c,d we depict the comparison between the spectra corresponding to the thermodynamic limit and to the truncated lattice. As can be observed from the figure, the spectra for the truncated lattice give a good approximation to the thermodynamic limit. It is worth mentioning that the spectra depicted in figures 2.c,d are plotted in logarithmic scale so to artificially enhance the discrepancy of the distance between the thermodynamic limit and the truncated lattice. The distance corresponding to these plots lies well below $\Delta S(T) < \exp(-7.5) \approx 5\times10^{-4}$. The convergence of the power spectrum is much faster than the one for the probability density (compare both scales in figures 1).

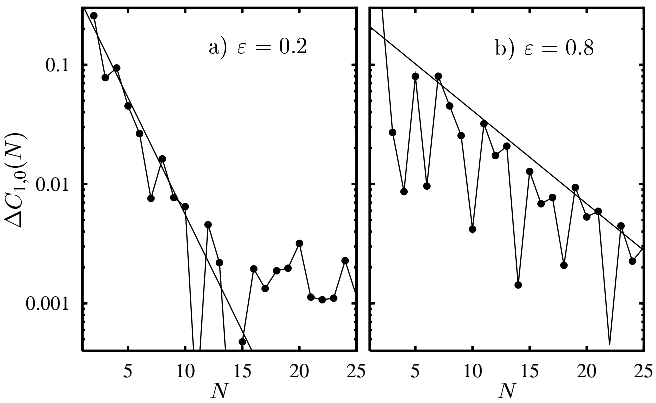


FIG. 3. Difference of the two-point correlation between the truncated lattice and the thermodynamic limit for two neighbours at the same iteration ($C(\xi = 1, \tau = 0)$).

To complete the comparison picture we compute the two-point correlation [9]

$$C(\xi,\tau) = \frac{\langle uv\rangle - \langle u\rangle\langle v\rangle}{\langle u^2\rangle - \langle u\rangle^2}, \tag{3}$$

where $u = x_i^t$ and $v = x_{i+\xi}^{t+\tau}$. Thus, $C(\xi,\tau)$ corresponds to the correlation of two points in the lattice dynamics separated by $\xi$ sites and $\tau$ time steps. To obtain the two-point correlation for the truncated lattice we consider the two points closest to the central site separated by $\xi$. We then compute $\Delta C_{\xi,\tau}(N)$ defined as the absolute value of the difference of the correlation in the thermodynamic limit with that obtained using the truncated lattice of size $N$. In figure 3 we plot $\Delta C_{1,0}(N)$ as a function of $N$ for $\varepsilon = 0.2$ and 0.8. For $\varepsilon = 0.2$, due to limited accuracy of our calculations, the saturation is reached around $N = 10$. Nonetheless it is possible to observe an exponential decrease (straight lines in the linear-log plot) before the saturation. For larger values of $\varepsilon$ the exponential convergence is more evident (see figure 3.b). Similar results were obtained for intermediate $\varepsilon$-values. Note that because the correlation oscillates, it is not possible to have a point by point exponential decay for $\Delta C_{1,0}(N)$, however, the upper envelope clearly follows an exponential decay (see straight lines for guidance). Similar results were obtained for different values of $(\xi,\tau)$.

The above comparisons were carried out by using the data produced by the known system (1). Often, in practice, one is deprived of the evolution laws of the system. In such cases, the only way to analyse the system is by using time series reconstruction techniques. This is particularly appropriate when dealing with real spatio-temporal systems where, typically, only a fraction of the set of variables can be measured or when the dynamics is only indirectly observed by means of a scalar measurement function. In the following we suppose that the only available data is provided by the time series of a set of variables in a small spatial region. We would like to study the effects on predictability when using a truncated lattice instead of the thermodynamic limit.

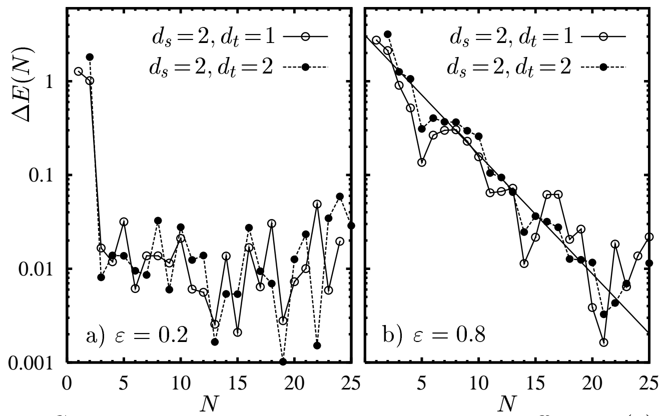


FIG. 4. Normalised one-step prediction error difference (5) between a truncated lattice and the thermodynamic limit for two spatio-temporal embeddings ($(d_s, d_t) = (2,1)$ and $(d_s, d_t) = (2,2)$) and different couplings strengths.

Instead of limiting ourselves to one-dimensional time-series (temporal embedding) we use a mix of temporal and spatial delay embeddings (spatio-temporal embedding) [2]. Therefore we use the delay map

$$\boldsymbol{X}_i^t = \left(\boldsymbol{y}_i^t, \boldsymbol{y}_{i-1}^t, \ldots, \boldsymbol{y}_{i-(d_s-1)}^t\right), \tag{4}$$

whose entries $\boldsymbol{y}_i^t = (x_i^t, x_i^{t-1}, \ldots, x_i^{t-(d_t-1)})$ are time-delay vectors and where $d_s$ and $d_t$ denote the spatial and temporal embedding dimensions. The overall embedding dimension is $d = d_s d_t$. The delay map (4) is used to predict $x_i^{t+1}$. Note that we are using spatial coordinates only from the left of $x_i^{t+1}$ (i.e. $x_j^t$ such that $j \le i$). An obvious choice of spatio-temporal delay would be a symmetric one such as $\boldsymbol{X}_i^t = (x_{i-1}^t, x_i^t, x_{i+1}^t)$. However, this would give artificially good results (for both the full and truncated lattices) since $x_i^{t+1}$ depends only on these variables (cf. (1)). This is an artefact of the choice of coupling and observable and could not be expected to hold in general. Therefore, we use the delay map (4) in order to "hide" some dynamical information affecting the future state and hence make the prediction problem a non-trivial one. The best one-step predictions [2] using the delay map (4) are typically obtained for $d_s = d_t = 2$. Here we use the two cases $(d_s, d_t) = (2,1)$

and $(d_s, d_t) = (2, 2)$; almost identical results are obtained for higher dimensional embeddings ($(d_s, d_t) \in [1, 4]^2$). Denote by $E(N)$ the normalised root-mean square error for the one step prediction using the delay map (4) at the central portion of the truncated lattice of size $N$. The comparison between $E(N)$ and $E(N \to \infty)$ is shown in figure 4 where we plot the absolute value of the normalised error difference

$$\Delta E(N) = |(E(N) - E(\infty))/E(\infty)| \tag{5}$$

for increasing $N$ and for different spatio-temporal embeddings and coupling strengths. The figure shows a rapid decay of the prediction error difference for small $N$ and then a saturation region where the limited accuracy of our computation hinders any further decay. For $\varepsilon = 0.2$ the drop to the saturation region is almost immediate while for the large coupling value $\varepsilon = 0.8$ the decay is slow enough to observe an apparently exponential decay (see fitted line corresponding to $d_s = d_t = 2$ for $N = 1, \ldots, 20$), thereafter the saturation region is again reached. For intermediate values of $\varepsilon$, the saturation region is reached between $N = 5$ and 20 (results not shown here). Before this saturation it is possible to observe a rapid (exponential) decrease of the normalised error difference. This corroborates again the fact that it seems impossible in practice to differentiate between the dynamics of the relatively small truncated lattice and the thermodynamic limit.

All the results in this letter where obtained from the simulation of a truncated lattice with white noise inputs at the boundaries. Other kinds of inputs did not change our observations in a qualitative way. It is worth mentioning that a truncated lattice with random inputs with the *same* probability density as the thermodynamic limit ($\rho_\infty(x)$) produces approximatively the same exponential decays as above with just a downward vertical shift (i.e. same decay but smaller initial difference).

The properties of the thermodynamic limit of a coupled logistic lattice we considered here (probability densities, power spectra, two-point correlations and predictability) were approximated remarkably well (exponentially close) by a truncated lattice with random inputs. Therefore, when observing data from a limited spatial region, given a finite accuracy in the computations and a reasonably small truncated lattice size, it would be impossible to discern any dynamical difference between the thermodynamic limit lattice and its truncated counterpart. The implications from a spatio-temporal systems time series perspective are quite strong and discouraging: even though in theory one should be able to reconstruct the dynamics of the *whole* attractor of a spatio-temporal system from a local time series (Takens theorem [10]), it appears that due to the limited accuracy (CPU precision, time and memory limitations, measurement errors, limited amount of data) it would be impossible to test for definite high-dimensional determinism in practice.

The evidence presented here suggests the impossibility of reconstructing the state of the whole lattice from localised information. It is natural to ask whether we can do any better by observing the lattice at many (possibly all) different sites. Whilst in principle this would yield an embedding of the whole high-dimensional system, it is unlikely to be much more useful in practice. This is because the resulting embedding space will be extremely high dimensional and any attempt to characterise the dynamics, or fit a model will suffer from the usual "curse of high dimensionality". In particular, with any realistic amount of data, it will be very rare for typical points to have close neighbours. Hence, for instance, predictions are unlikely to be much better than those obtained from just observing a localised part of the lattice.

If one actually wants to predict the behaviour at many or all sites, our results suggest that the best approach is to treat the data as coming from a number of uncoupled small noisy systems [11], rather than a single large system. Of course, if one has good reason to suppose that the system is spatially homogeneous, one should fit the same local model at all spatial locations, thereby substantially increasing the amount of available data.

This work was carried out under an EPSRC grant (GR/L42513). JS would also like to thank the Leverhulme Trust for financial support.

---

* E-mail: R.Carretero@ucl.ac.uk
† URL: http://www.ucl.ac.uk/CNDA

[1] H. Kantz and T. Schreiber, *Nonlinear Time Series Analysis* (Cambridge University Press, 1998).
[2] S. Ørstavik and J. Stark, Phys. Lett. A **247** (1998) 146.
[3] K. Kaneko, Prog. Theor. Phys. **72**, 3 (1984) 480; R. Kapral, Phys. Lett. A **31**, 6 (1985) 3868.
[4] A. Pikovsky and J. Kurths, Physica D **76** (1994) 411.
[5] R. Carretero-González *et al.*, *Scaling and interleaving of sub-system Lyapunov exponents for spatio-temporal systems.* To appear Chaos **9** (1999). Preprint version: http://www.ucl.ac.uk/∼ucesrca/abstracts.html.
[6] N. Parekh, V.R. Kumar and B.D. Kulkarni, Chaos **8**, 1 (1998) 300.
[7] D. Ruelle, Commun. Math. Phys. **87** (1982) 287; K. Kaneko, Prog. Theor. Phys. **99** (1989) 263.
[8] A. Lemaître, H. Chaté and P. Manneville, Europhys. Lett. **39**, 4 (1997) 377.
[9] T. Schreiber, J. Phys. A **23** (1990) L393.
[10] F. Takens, Lecture Notes in Math. **898** (1981) 366.
[11] For a generalisation on embedding forced and stochastic systems please see: J. Stark *et al.*, Nonlinear Analysis **30** (1997) 5303.